Endogenous Opioid Release in the Human Brain Reward System Induced by Acute Amphetamine Administration

Supplementary Information

Table S1. Demographic characterization and injected tracer doses for the two treatment groups.

Parameters	**High Dose Amphetamine 0.5 mg/kg *n* = 6**	**Ultra-low Dose Amphetamine ≅ 0.017 mg/kg *n* = 6**
	Mean (SD)	
Age (years)	36.5 (11.9)	42 (5.5)
Weight (Kg)	72.6 (7.4)	83.3 (14.4)
BDI Total Score	0.2 (0.4)	2 (3.2)
BIS Total Score	10.33 (1.8)	10 (1.7)
EPQR		
Extraversion	15.5 (2.4)	15.2 (5)
Psychoticism	3 (1.9)	3.7 (1.5)
Neuroticism	3.67 (2.42)	4.5 (3.9)
Lie factor	13.5 (4.3)	11 (4.4)
Baseline PET Scan		
Injected Activity (MBq)	211.8 (78.3)	299.6 (40.8)*
Injected Mass (µg)	0.47 (0.34)	1.04 (1.14)*
Post-amphetamine PET Scan		
Injected Activity (MBq)	223 (95.9)	276.3 (48.2)
Injected Mass (µg)	0.55 (0.38)§	1.13 (0.15)*

BDI, Beck Depression Inventory; BIS, Barratt Impulsivity Scale; EPQR: Eysenck Personality Questionnaire-Revised version; MBq: megabecquerel; PET, positron emission tomography.

High Dose: 0.5 mg/kg amphetamine; Ultra-Low Dose: 1.25 mg *or* 0.017 mg/kg.

§ $p < 0.05$ vs Baseline PET scan injected mass.

* $p < 0.05$ vs High Dose Amphetamine group.

Table S2. [^{11}C]carfentanil BP_{ND} at baseline (Base) and Post-amphetamine (PA), in subjects receiving high (H1-H6) and ultra-low (UL1-UL6) amphetamine doses, in each region of interest.

Subject Scans	**FL**	**Insula**	**AC**	**Cau**	**Put**	**VST**	**Amy**	**Tha**	**HT**	**PAG**
H1 Base	1.20	1.55	1.64	1.68	1.82	3.09	1.74	2.29	1.91	1.24
H1 PA	1.13	1.44	1.48	1.53	1.66	2.63	1.55	2.19	2.00	1.13
H2 Base	0.99	1.29	1.47	0.54	1.63	2.34	1.44	1.30	1.19	0.79
H2 PA	0.93	1.17	1.37	0.45	1.48	2.24	1.43	1.16	1.12	0.79
H3 Base	1.03	1.24	1.36	1.28	1.66	2.55	1.49	1.75	1.74	0.95
H3 PA	0.97	1.21	1.32	1.18	1.51	2.45	1.45	1.65	1.55	0.96
H4 Base	1.02	1.34	1.45	1.07	1.71	2.71	1.76	1.93	2.36	1.49
H4 PA	0.95	1.27	1.33	0.96	1.57	2.49	1.85	1.71	1.95	1.30
H5 Base	0.98	1.38	1.42	1.22	1.56	2.61	1.92	2.15	2.37	1.42
H5 PA	0.90	1.27	1.34	1.09	1.44	2.38	1.78	1.94	2.40	1.31
H6 Base	1.03	1.35	1.33	1.57	1.87	2.65	1.73	1.99	1.70	0.97
H6 PA	0.94	1.24	1.24	1.45	1.74	2.71	1.79	1.91	1.54	0.95
Mean BP_{ND} HD Base	1.04	1.36	1.44	1.23	1.71	2.66	1.68	1.90	1.88	1.14
Mean BP_{ND} HD PA	0.97 *	1.27 *	1.35 *	1.11 *	1.57 *	2.49	1.64	1.76 *	1.76	1.07
Mean ΔBP_{ND} HD %	7.0 †	6.7 §	6.5 §	10.2 §	8.4 †	6.2 §	2.1	7.5 †	6.2	5.2
UL1 Base	1.33	1.55	1.72	1.75	1.90	2.88	1.63	2.14	2.03	1.32
UL1 PA	1.41	1.64	1.83	1.86	2.00	2.97	2.00	2.30	1.90	1.48
UL2 Base	1.35	1.57	1.66	1.40	1.89	2.89	1.79	1.93	2.03	0.92
UL2 PA	1.26	1.51	1.56	1.25	1.80	2.86	1.84	1.89	1.89	0.81
UL3 Base	1.10	1.42	1.47	1.72	1.91	2.70	1.86	2.13	1.85	1.17
UL3 PA	1.13	1.41	1.49	1.81	1.97	2.78	1.96	2.18	1.85	1.18
UL4 Base	1.02	1.47	1.37	1.76	1.87	2.78	2.10	2.34	1.94	1.14
UL4 PA	0.94	1.37	1.27	1.59	1.76	2.69	1.85	2.27	1.70	1.09
UL5 Base	0.92	1.28	1.25	1.57	1.68	2.47	1.82	1.78	1.70	0.91
UL5 PA	0.89	1.20	1.18	1.42	1.62	2.35	1.67	1.67	1.53	0.81
UL6 Base	0.97	1.19	1.31	1.53	1.62	2.47	1.64	1.83	1.82	1.14
UL6 PA	0.97	1.22	1.33	1.51	1.59	2.42	1.68	1.86	1.73	1.16
Mean BP_{ND} ULD Base	1.11	1.41	1.46	1.62	1.81	2.70	1.81	2.03	1.89	1.10
Mean BP_{ND} ULD PA	1.10	1.39	1.44	1.57	1.79	2.68	1.83	2.03	1.77 °	1.09
Mean ΔBP_{ND} ULD %	1.5	1.6	1.7	3.3	1.3	0.8	-2.3	0.0	6.7	2.1

FL, frontal lobe; AC, anterior cingulate; Cau, caudate; Put, putamen; VST, ventral striatum; Amy, amygdala; Tha, thalamus; HT, hypothalamus; PAG, periaqueductal gray.

* $p < 0.005$ vs Baseline BP_{ND} High-Dose.

° $p < 0.05$ vs Baseline BP_{ND} Ultra Low-Dose.

† $p \leq 0.01$ vs ΔBP_{ND} Ultra Low-Dose.

§ $p < 0.09$ vs ΔBP_{ND} Ultra Low-Dose.

Table S3. Statistical summaries of main anatomical clusters in Figure 2 reporting differences in [^{11}C]carfentanil ΔBP_{ND} between high and ultra-low amphetamine dose groups ($\Delta BP_{ND\ high} > \Delta BP_{ND\ ultra\text{-}low}$). For each cluster we report the lateralization (Lat), the total number of voxels (N. voxels) that pass significance, and the T-statistics (T_Max) and the Montreal Neurological Institute coordinates of the main peaks within the cluster.

			Peaks			
Localization of clusters	**Lat**	**N. voxels**	**T_Max**	**X**	**Y**	**Z**
Putamen, Nucleus Accumbens, OrbitoFrontal Cortex	R	1947	3.63	26	13	-1
			3.63	32	5	-1
			3.37	11	6	-7
			3.37	16	11	-14
			3.08	21	14	4
			3.08	27	-3	4
Frontal Lobe (Inferior and middle frontal gyri, precentral gyrus)	R	1394	4.06	48	16	27
			3.88	47	6	35
			3.60	45	17	32
			3.19	49	1	33
			2.83	47	24	32
			2.73	49	25	29
Middle Frontal Gyrus	L	884	3.65	-19	3	60
			3.43	-24	4	45
			3.38	-23	2	46
			3.07	-28	1	53
			2.85	-28	-4	53
Middle Frontal Gyrus	R	816	4.01	31	33	33
			3.47	43	21	36
			3.34	45	26	35
			2.75	36	29	39
Middle Frontal Gyrus	L	512	3.49	-44	21	29
			3.27	-40	27	33
			2.93	-47	26	37
Middle Frontal Gyrus	R	499	3.87	30	0	51
			3.65	31	1	54
			3.49	25	-2	45
			3.36	23	0	57
			3.24	35	0	55
			3.16	36	-3	54
Middle Frontal Gyrus	R	304	3.12	38	49	25
			2.52	35	40	32
Inferior Frontal Gyrus	L	281	3.57	-52	7	31
			2.52	-50	12	29
Precentral Gyrus	L	202	3.95	-40	-3	34
Middle Frontal Gyrus	R	185	3.52	46	3	47
Superior Frontal Gyrus	R	146	3.30	20	44	39
Precentral –Postcentral Gyri	L	124	3.61	-42	-20	57
Caudate	R	61	3.02	14	2	22
Precentral gyrus	R	59	3.34	30	-13	52
Thalamus	R	40	3.16	15	-7	13

L, left; R, right.

Table S4. Vital parameters (heart rate, systolic and diastolic blood pressure) at different time points relative to amphetamine administration (-3 h; 0 h; +3 h; +6 h). At the post-amphetamine time points (+3 h and +6 h post-amphetamine), significant increases from baseline were observed only in the high dose group (* $p < 0.05$). Between-groups differences were significant for changes over time in heart rate ($p < 0.0001$), and systolic blood pressure ($p < 0.05$), but not for diastolic blood pressure ($p = 0.07$).

		Hours Relative to Amphetamine Administration			
				post-amphetamine time points	
Mean (SD)	**Amphetamine Dose Group**	**-3**	**0**	**+3**	**+6**
Heart rate bpm	High dose	63.00 (6.32)	57.00 (5.44)	81.33 (9.00)*	86.67 (14.93)*
	Ultra-Low dose	64.17 (8.38)	56.33 (8.40)	70.83 (6.65)	64.50 (7.26)
Systolic BP mmHg	High dose	122.50 (6.22)	128.00 (7.24)	135.50 (5.24)*	136.33 (8.24)*
	Ultra-Low dose	120.83 (8.08)	121.50 (9.54)	120.67 (6.31)	124.33 (7.12)
Diastolic BP mmHg	High dose	72.67 (4.68)	80.00 (10.71)	82.33 (11.11)	81.17 (8.13)*
	Ultra-Low dose	75.00 (7.90)	79.00 (7.95)	71.67 (5.00)	75.17 (3.87)

BP, blood pressure; bpm, beats per minute.

Table S5. Affinity of endogenous opioid peptides for μ-opioid receptors (MOR).

	Affinity (nM)			
Opioid peptide	**Human cloned MOR**	**Rat brain membranes**	**Radioligand**	**References**
β-endorphin	0.94 - 1.6	4.4	[^{3}H]DAMGO	Raynor *et al.* 1994 (1); Raynor *et al.* 1995 (2); Toll *et al.* 1998 (3); Zadina *et al.* 1997 (4)
Leu-enkephalin	3.4 - 7.4		[^{3}H]DAMGO	Raynor *et al.* 1994 (1); Raynor *et al.* 1995 (2); Toll *et al.* 1998 (3)
Met-enkephalin	0.65	5.9	[^{3}H]DAMGO	Raynor *et al.* 1994 (1); Zadina *et al.* 1997 (4)
Dynorphin A	32		[^{3}H]DAMGO	Raynor *et al.* 1994 (1)
Dynorphin B	3		[^{3}H]DAMGO	Toll *et al.* 1998 (3)
Endomorphin-1		0.36	[^{3}H]DAMGO	Zadina *et al.* 1997 (4)
Endomorphin-2		0.69	[^{3}H]DAMGO	Zadina *et al.* 1997 (4)

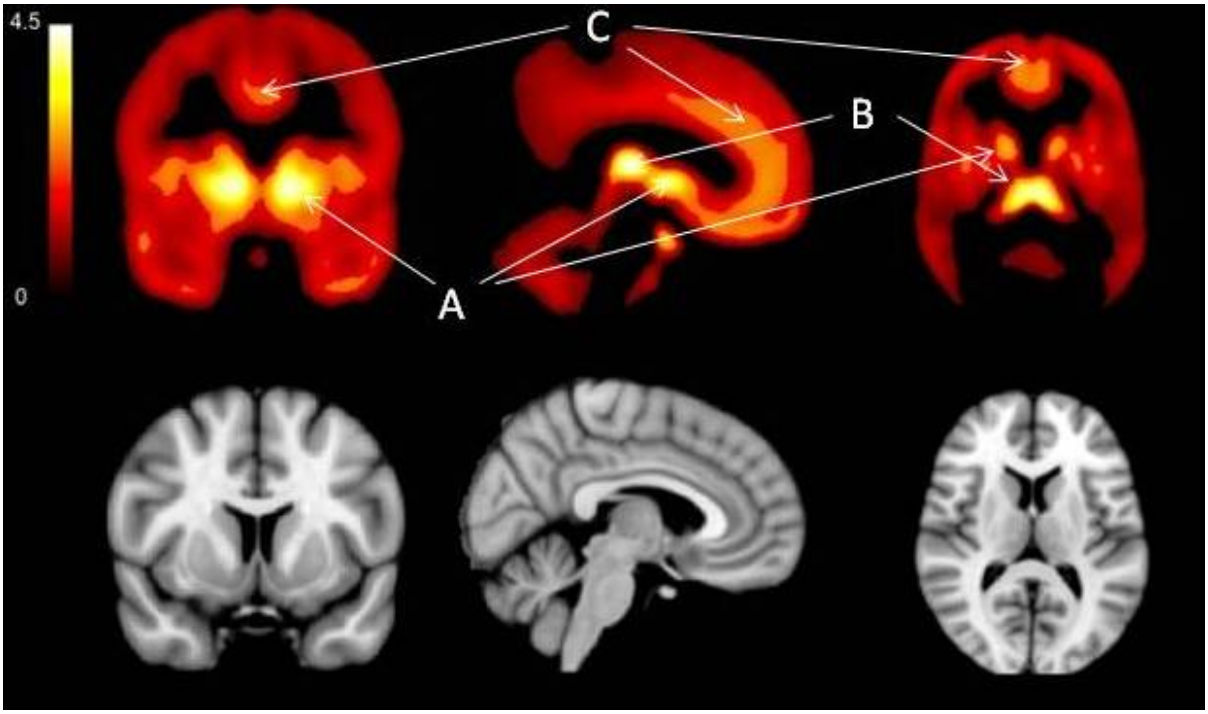

Figure S1. Distribution of [^{11}C]carfentanil binding to μ-opioid receptors in human brain. Top panel: parametric map of average of baseline BP_{ND} from all 12 subjects. Areas with high radiotracer binding: Striatopallidal regions (including nucleus accumbens, caudate, and putamen, indicated by A), thalamus (indicated by B), and cingulate cortex (indicated by C). Bottom panel: Montreal Neurological Institute template brain.

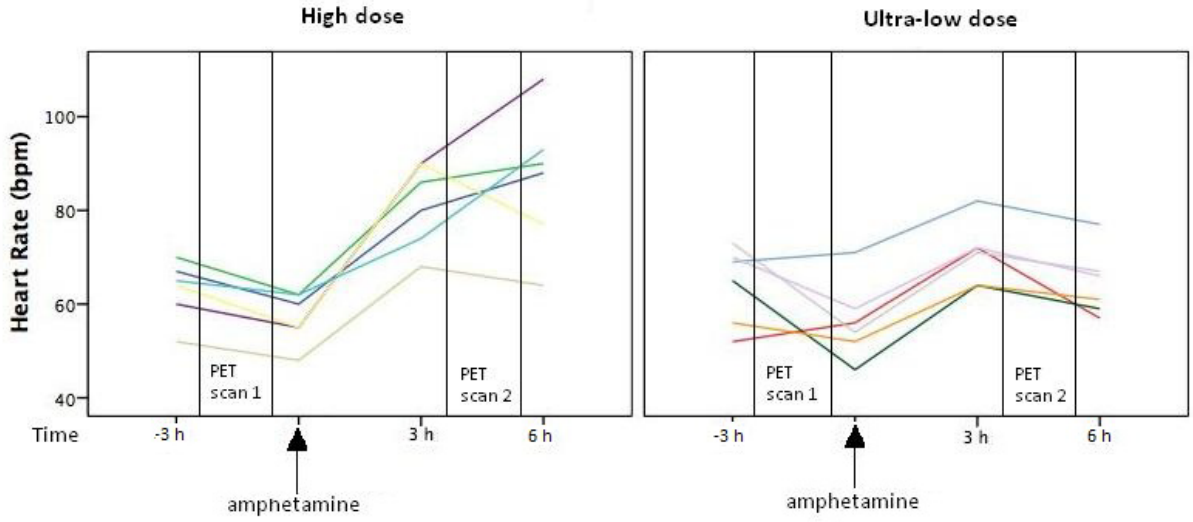

Figure S2. Heart rate changes in response to amphetamine administration across the groups. The changes in heart rate over time were significantly different between groups ($p < 0.0001$). There were significant group differences in the within-subjects contrasts between post-amphetamine time points (+3 h and +6 h) and baseline (0 h). At 3 h and 6 h post – amphetamine administration, a significant heart rate increase was observed only in the high dose group ($p < 0.01$). bpm, beats per minute; PET, positron emission tomography.

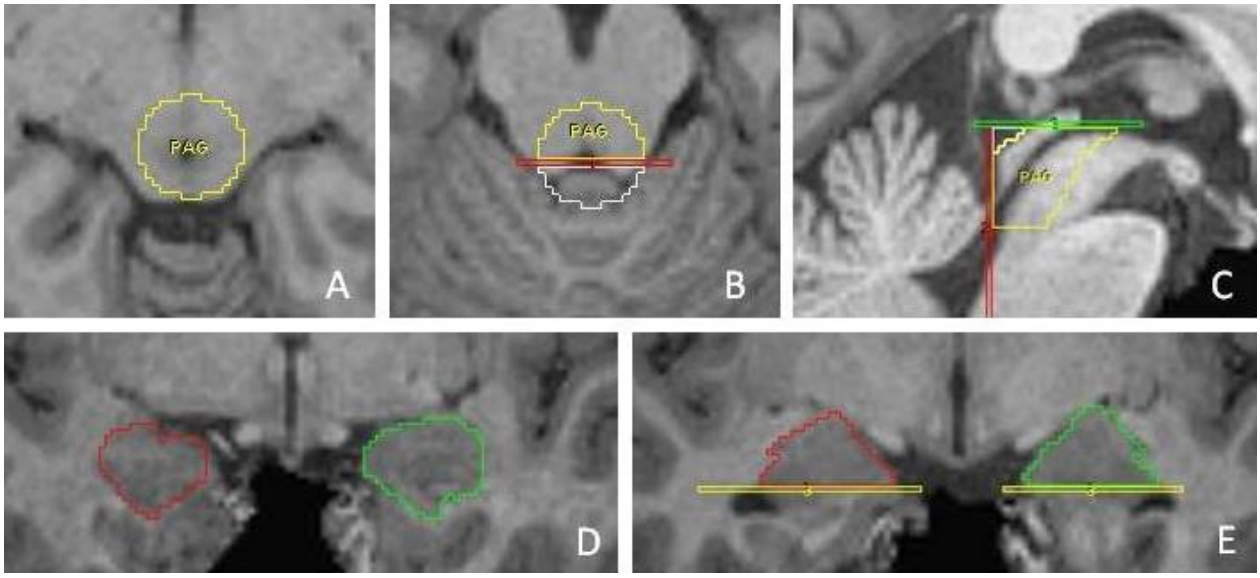

Figure S3. Manual definition of periaqueductal gray (PAG) and amygdala. **(A-C)** Definition of PAG. On the axial view PAG is defined as a circle centered in the cerebral aqueduct **(A)**. We deleted the portion of PAG (**B**, white circle) that lies posterior to a line (**C**, red line) passing through the most anterior border of the cerebellum on the medial sagittal slice **(C)**. **(D-E)** Amygdalae are defined on coronal slices **(D)**. Only gray matter above a horizontal line (in yellow) passing through the superior edge of the temporal horn of the lateral ventricle is classified as amygdala **(E)**. Further details are in the text.

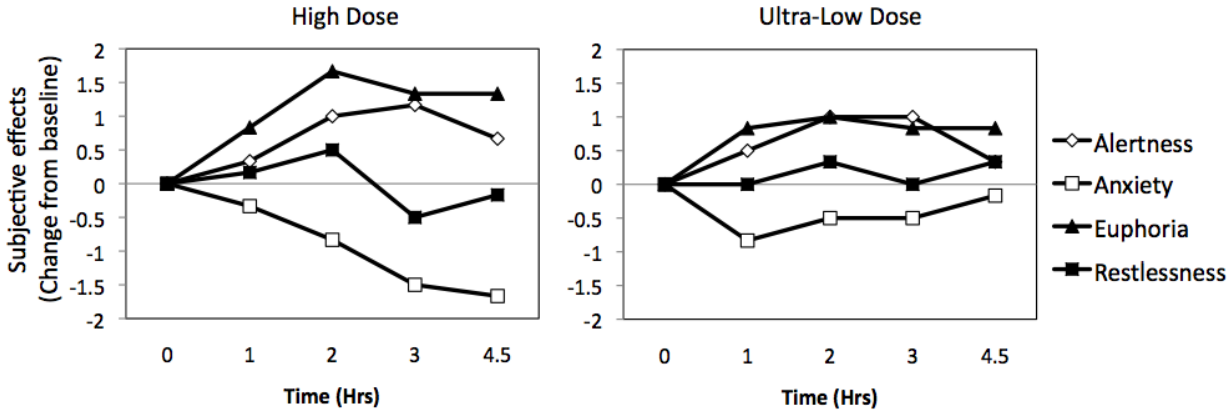

Figure S4. Changes in ratings of subjective dimensions (alertness, anxiety, euphoria, and restlessness) in response to amphetamine administration across the groups. Repeated-measures analysis of variance indicated that decrease in anxiety in the high-dose group approached statistical significance ($p = 0.051$), and there was a significant effect of the Time X Group interaction for ratings of anxiety ($p < 0.05$). Increases in euphoria and alertness were not significant in both dose groups, and no significant effect of the Time X Group interaction was observed. Ratings of restlessness indicated no change from baseline in any of the groups.

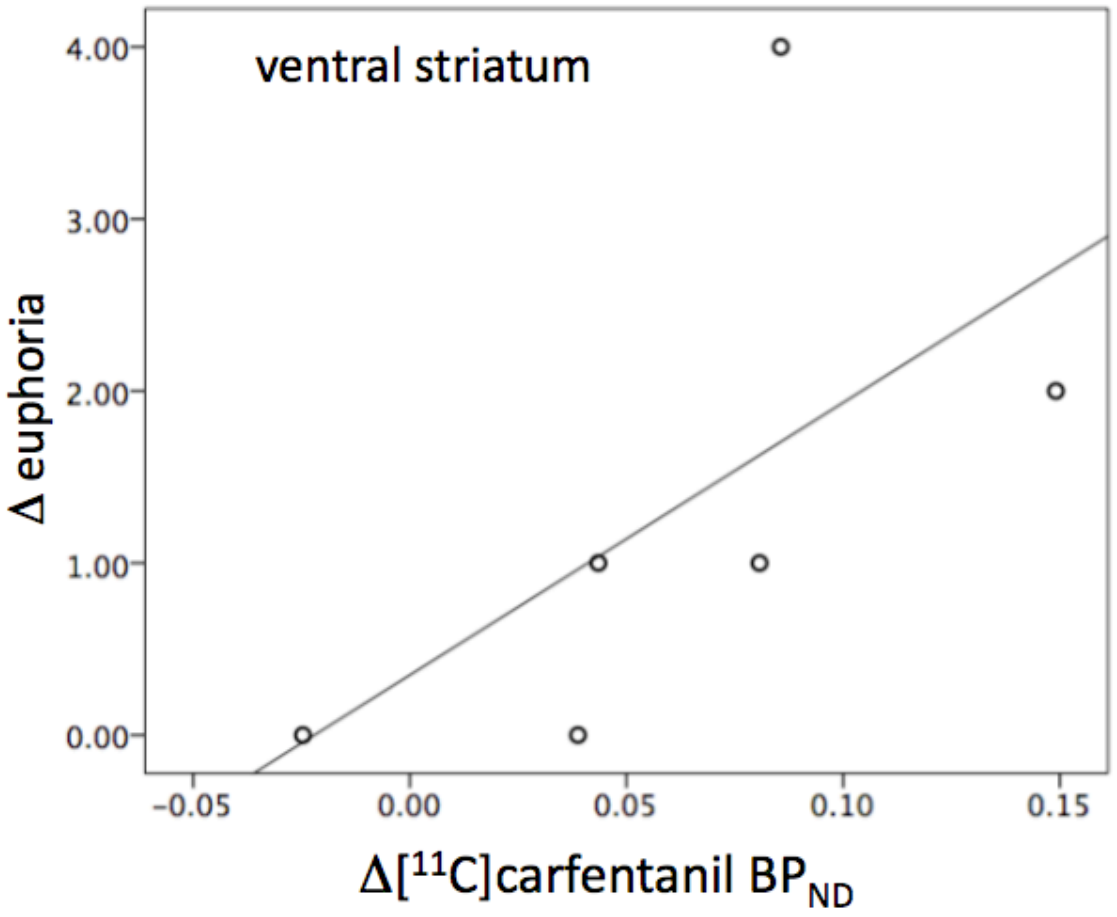

Figure S5. Relationship between regional Δ[^{11}C]carfentanil BP_{ND} in the ventral striatum and changes in ratings of euphoria. Δeuphoria scores represent the differences between rating scores at 3 h after amphetamine administration and the baseline rating scores. The correlation of Δeuphoria to ΔBP_{ND} in the ventral striatum (Spearman's $\rho = 0.91$; $p = 0.01$) is consistent with the notion that the euphoric effects of amphetamine are mediated by release of endogenous opioids.

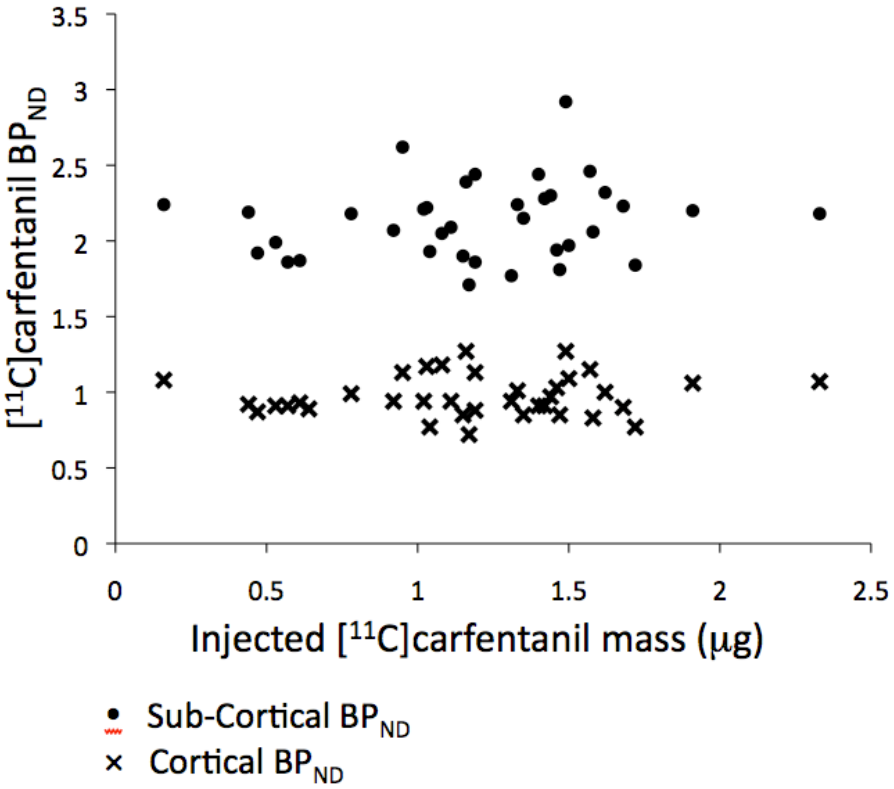

Figure S6. Relationship between injected [^{11}C]carfentanil BP_{ND} in cortical and subcortical regions and injected mass in 37 subjects examined with [^{11}C]carfentanil positron emission tomography in the Clinical Imaging Centre over 2 years. No correlation was observed between the injected mass and [^{11}C]carfentanil BP_{ND}, indicating that the doses of injected carfentanil used in our study result in occupancy of the μ-opioid receptors in the tracer range.

Supplementary Methods

Subjects

The demographic and methodological parameters for all participants are presented in Table S1. The study was performed at the Clinical Imaging Centre, Hammersmith Hospital, after approval by the Essex 1 Research Ethics Committee and the Administration of Radioactive Substances Advisory Committee. All subjects provided informed written consent according to Good Clinical Practice guidelines.

Volunteers were recruited from a database of healthy volunteers and they were paid for their participation in the study. Inclusion criteria were non-smoking males aged between 25 and 55 years. Exclusion criteria were a positive pre-study alcohol/drug screening, a history of drug abuse or dependence, any concomitant medications, the presence of past or present neurological or medical illnesses, including gastro-intestinal, cardiovascular, and endocrine disorders and body mass index above 31.0 kg/m^2. Subjects were also excluded if they had any present or past psychiatric disease as assessed by a psychiatrist through a semi-structured psychiatric interview, or if they presented any depressive symptoms [Beck Depressive Inventory (BDI) > 9]. Clinical status was assessed by history, review of systems, physical examination, routine blood tests, urine analysis, and electrocardiogram.

Previous research indicated that depressive symptoms, impulsivity and personality traits are associated to an alteration of the endogenous opioid system (5-7). To control for these potential confounding factors, impulsivity and personality traits were measured at screening in all subjects using the BDI, Barratt Impulsivity Scale (BIS) and Eysenck Personality Questionnaire-Revised version (EPQR). Subjects in the two amphetamine dose groups were well-matched with regard to the demographic characteristics, as well as BDI, BIS, and EPQR scores (See Table S1).

[^{11}C]carfentanil Synthesis

The radiotracer [^{11}C]carfentanil was synthesised by reaction of [^{11}C]methyliodide with the desmethyl precursor using a modified method previously described (8). [^{11}C]carbon dioxide was produced using an Eclipse RDS cyclotron (Siemens, Washington, DC) by the ^{14}N(p,α)^{11}C reaction and 18 MeV proton irradiation (typical bombardment of 55 µA, 50 min) of nitrogen gas containing 1% oxygen. [^{11}C]carbon dioxide was transformed to [^{11}C]methyliodide using a GE Microlab (GE GEMS, Uppsala, Sweden). A semi-automated Modular Lab Multifunctional Synthetic Module (Eckert & Ziegler, Germany) was configured to perform the different steps of the radiosynthesis from this stage.

The [^{11}C]methyliodide was transferred to the Modular Lab module and trapped in a 5 ml vial containing 0.5 mg of precursor desmethyl carfentanil and 3 µl tetrabutylammonium hydroxide (0.1 M in methanol) in 350 µl dimethylformamide (DMF) cooled down at -5°C. The resulting reaction mixture was heated for 5 min at 70°C to form [^{11}C]carfentanil. The reaction mixture was diluted in 5 ml wash solution (87% water, 10% 1-propanol and 3% 5 M ammonium hydroxide) and loaded onto a Waters Sep Pak tC2 cartridge (Waters, Milford, MA). The cartridge was washed with a further 10-mL of the wash solution followed by 25 mL water. The purified [^{11}C]carfentanil was eluted from the cartridge with 1 mL ethanol. The cartridge was further eluted with 10 ml of 0.9% saline solution to lead to [^{11}C]carfentanil formulated in 11 mL of 10% (v/v) ethanol in 0.9% saline solution for injection. The resulting solution was passed through a 0.2 µm sterile filter (Acrodisc, sterile, 25 mm, 0.22 µm, Pall, Port Washington, NY) into its final sterile container.

The standard carfentanil was obtained from Advanced Biochemical Compounds (Radeberg, Germany). The precursor, desmethyl carfentanil, was obtained from Pharmasynth (Tartu, Estonia).

Manual Definition of Periaqueductal Gray (PAG) and Amygdala

The PAG was manually defined on the axial slices, starting with the slices inferior to the most inferior axial slice where the posterior commissure can be seen (Figure S3, A). A circle of 14 mm diameter was centered at the center of the cerebral aqueduct. The inferior limit was defined where the 4^{th} ventricle comes into view (Figure S3, B). The posterior border was defined on the medial sagittal slice by drawing a vertical line which passes through the most anterior border of the cerebellum (Figure S3, C). The portion of the circle on the axial slices that lies posterior that border has been deleted (Figure S3, B).

The amygdala was manually defined on each subject's magnetic resonance image following the guidelines obtained by the Columbia Positron Emission Tomography (PET) group. Briefly, the amygdala was defined on the coronal plane on all the slices where its dense gray matter could be seen (Figure S3, D). When the temporal horn of the lateral ventricle comes into view a horizontal line is drawn medially from its most superior edge on each slice. Gray matter above the line is classified as amygdala (Figure S3, E).

Voxel-level Analysis

Whole-brain BP_{ND} images were generated using the basis function implementation of the SRTM (9), with kinetic time constants ranging from 0.0008 to 0.01 s^{-1}, and normalized to the MNI152 template (http://www2.bic.mni.mcgill.ca) using SPM5b (Wellcome Trust Centre for Neuroimaging, http://www.fil.ion.ucl.ac.uk/spm). These images were analyzed to seek brain regions where ΔBP_{ND} significantly differed between the high and ultra-low dose groups. For this purpose, we employed a random-effects nonparametric permutation testing procedure (10), with $5x10^3$ permutations and an 8 mm variance smoothing (as implemented in the FSL function Randomise, http://www.fmrib.ox.ac.uk/fsl). This analysis allows computation of a two-sample *t*-test featuring permutation-based inference. The main

advantages of permutation testing in the current context is that we can account for multiple comparisons (~10^6 voxels were tested), that the underlying "null" distribution of data need not be known in advance, and that we can compensate for low degrees of freedom (small numbers of subjects) when spatial variance smoothing is employed. Regions of significant effects resulting from these regressions were defined using cluster-mass thresholding ($z = 2.3$, $p < 0.05$) correction for full-brain family-wise error (FWE). Normalized voxels displaying zero signal in at least one individual scan session, or falling below a 30% threshold of containing gray matter based on a study population-specific probabilistic atlas calculated using FAST [part of FSL (11)], were excluded from statistical testing.

In Vitro Binding Study

To determine the affinity of amphetamine at [^{11}C]carfentanil labeled μ-opioid receptors (MOR) receptors, K_i values were generated using *in vitro* homogenate binding. Briefly, rat whole brain minus cerebellum membranes were generated and diluted to a protein concentration of 1 mg/ml in assay buffer (50 mM Tris HCl, 140 mM NaCl, 5 mM KCl, 1.5 mM $MgCl_2$, 1.5 mM $CaCl_2$, pH 7.4, 37^{o}C). A range of amphetamine concentrations (100 μM-10 pM) were used to displace a fixed concentration of [^{11}C]carfentanil. Specific binding was determined using naloxone (10 μM). The final volume for each assay was 500 μl. Each data point was performed in triplicate. Following incubation (30 minutes, 37°C), the assay was terminated by filtration through Whatman glass fibre (GF/B; Piscataway, NJ) filters pre-soaked in 0.05% polyethyleneimine with ice-cold wash buffer (50 mM Tris HCl, 1.4 mM $MgCl_2$, pH 7.4 at 4°C). K*d* values, previously determined with [^{11}C]carfentanil, were used to generate K_i values using the method of Cheng and Prusoff (12).

Supplementary Discussion

The change in subjective rating of euphoria, induced by amphetamine administration, was positively correlated with the reduction in [^{11}C]carfentanil in the ventral striatum (Figure S5). Although limited by the small sample size, these findings may indicate that the subjective effects are mediated via endogenous opioid release in the relevant brain regions. However, it is also possible that amphetamine might increase release of opioids and cause euphoria through unrelated actions. Clinical data support our interpretation indicating that the administration of an opioid antagonist attenuates the subjective effects of amphetamine (13). Also, PET studies in humans have shown amphetamine-induced ventral striatal dopamine release to correlate with the magnitude of the hedonic response to amphetamine (14-16). Our finding of a positive correlation between [^{11}C]carfentanil displacement in the ventral striatum and euphoric effects of amphetamine is consistent with the idea that MOR located in the ventral striatum play a central role in mediating the hedonic and rewarding properties of multiple drugs of abuse, as well as food and sexual stimuli (for review see (17)).

Berridge and Robinson distinguished the motivational aspects of the hedonic response, attributed to ventral striatal dopamine (DA) release, and the pleasurable aspects, attributed to ventral striatal MOR neurotransmission (18,19). The data in this paper would support the notion that the neural circuits responsible for motivational and pleasurable aspects of the hedonic responses may be closely intertwined in the brain (18), and that ventral striatal DA may drive both the *wanting* aspects by direct effects and *liking* aspects by indirect effects on opioid neurotransmission.

Our findings are also consistent with rodent data showing that infusion of MOR antagonists in the ventral striatum attenuates the rewarding effects of systemically administered cocaine (20). Taken together, these findings suggest that the dopamine and

opioid system have synergistic effects in mediating the subjective response to psychostimulants.

Our findings are limited by the small size of our sample. A confirmation in a larger cohort is therefore warranted.

Another possible methodological limitation is the choice of a method based on a reference region (SRTM) for the quantification of the BP_{ND} instead of direct measurement of the arterial plasma input function. Although it improves tolerability and safety for study participants, the use of a reference region can lead to a small bias if there is any specific binding in the reference region. While non-specific binding would not be expected to change following our pharmacological challenge, a small amount of specific binding in the reference region could be potentially affected by amphetamine. An examination of the occipital lobe time activity curves (TACs) demonstrates a slightly lower standardized uptake value (SUV) post-amphetamine than at baseline, for most of the subjects. No subject in our study has demonstrated an increase in occipital lobe SUV following amphetamine. Since arterial blood data were not acquired in this study, it is impossible to establish whether differences in occipital lobe TACs are a result of changes in the tissue characteristics (e.g. displacement of a small specific signal), or some peripheral effect acting through the plasma input (e.g. metabolism of the radiotracer). However, the direction of change in the occipital lobe TAC (reduction post-amphetamine) indicates that any possible bias incurred would make our results more conservative, and reduce our ability to see a reduction in BP_{ND} in the region of interest.

Supplemental References

1. Raynor K, Kong H, Chen Y, Yasuda K, Yu L, Bell GI, Reisine T (1994): Pharmacological characterization of the cloned kappa-, delta-, and mu-opioid receptors. *Mol Pharmacol.* 45:330-334.
2. Raynor K, Kong H, Mestek A, Bye LS, Tian M, Liu J, Yu L, Reisine T (1995): Characterization of the cloned human mu opioid receptor. *J Pharmacol Exp Ther.* 272:423-428.
3. Toll L, Berzetei-Gurske IP, Polgar WE, Brandt SR, Adapa ID, Rodriguez L, *et al.* (1998): Standard binding and functional assays related to medications development division testing for potential cocaine and opiate narcotic treatment medications. *NIDA Res Monogr.* 178:440-466.
4. Zadina, JE, Hackler, L, Ge, LJ, Kastin, AJ (1997): A potent and selective endogenous agonist for the mu-opiate receptor. *Nature.* 386:499-502.
5. Kennedy SE, Koeppe RA, Young EA, Zubieta JK (2006): Dysregulation of endogenous opioid emotion regulation circuitry in major depression in women. *Arch Gen Psychiatry.* 63:1199-1208.
6. Love TM, Stohler CS, Zubieta JK (2009): Positron emission tomography measures of endogenous opioid neurotransmission and impulsiveness traits in humans. *Arch Gen Psychiatry*. 66:1124-1134.
7. Williams TM, Davies SJC, Taylor LG, Daglish MR, Nutt DJ, Lingford-Hughes A (2008): Can personality traits elucidate the relationship between substance dependence and opioid receptor availability? *Eur Neuropsychopharmacol.* 18:S536.
8. Jewett DM (2001): A simple synthesis of [11C]carfentanil using an extraction disk instead of HPLC. *Nucl Med Biol.* 28:733-734.
9. Gunn RN, Lammertsma AA, Hume SP, Cunningham VJ (1997): Parametric imaging of ligand receptor binding in PET using a simplified reference region model. *Neuroimage.* 6:279-287.
10. Nichols TE, Holmes AP (2002): Nonparametric permutation tests for functional neuroimaging: a primer with examples. *Hum Brain Mapp.* 15:1-25.
11. Zhang Y, Brady M, Smith S (2001): Segmentation of brain MR images through a hidden Markov random field model and the expectation-maximization algorithm. *IEEE Trans Med Imaging.* 20:45-57.

12. Cheng Y, Prusoff WH (1973). Relationship between the inhibition constant (K1) and the concentration of inhibitor which causes 50 per cent inhibition (I50) of an enzymatic reaction. *Biochem Pharmacol.* 22:3099-3108.
13. Jayaram-Lindstrom N, Wennberg P, Hurd YL, Franck J (2004): Effects of naltrexone on the subjective response to amphetamine in healthy volunteers. *J Clin Psychopharmacol*. 24:665-669.
14. Martinez D, Slifstein M, Broft A, Mawlawi O, Hwang DR, Huang Y, *et al.* (2003): Imaging human mesolimbic dopamine transmission with positron emission tomography. Part II: amphetamine-induced dopamine release in the functional subdivisions of the striatum. *J Cereb Blood Flow Metab*. 23:285-300.
15. Abi-Dargham A, Kegeles LS, Martinez D, Innis RB, Laruelle M (2003): Dopamine mediation of positive reinforcing effects of amphetamine in stimulant naive healthy volunteers: results from a large cohort. *Eur Neuropsychopharmacol*. 13:459-468.
16. Drevets WC, Gautier C, Price JC, Kupfer DJ, Kinahan PE, Grace AA, *et al.* (2001): Amphetamine-induced dopamine release in human ventral striatum correlates with euphoria. *Biol Psychiatry*. 49:81-96.
17. Le Merrer J, Becker JA, Befort K, Kieffer BL (2009): Reward processing by the opioid system in the brain. *Physiol Rev*. 89:1379-1412.
18. Berridge KC, Robinson TE (1998): What is the role of dopamine in reward: hedonic impact, reward learning, or incentive salience? *Brain Res Rev.* 28:309-369.
19. Berridge KC, Robinson TE (2003): Parsing reward. *Trends Neurosci*. 26:507-513.
20. Soderman AR, Unterwald EM (2008): Cocaine reward and hyperactivity in the rat: sites of mu opioid receptor modulation. *Neuroscience*. 154:1506-1516.